1,4,5,8-Naphthalenetetracarboxylic dianhydride as transparent electron transport material in organic p-i-n solar cells

C. Falkenberg[a], C. Uhrich[b], B. Maennig[b], M. K. Riede[a], K. Leo[a]

[a]Institut für Angewandte Photophysik, TU Dresden, George-Bähr-Straße 1, 01069 Dresden, Germany;

[b]Now: Heliatek GmbH, Liebigstraße 26, 01187 Dresden, Germany

ABSTRACT

The transparent electron transport material NTCDA (1,4,5,8-naphthalenetetracarboxylic dianhydride) was examined in order to find a suitable substitute for C_{60} which is today often used in small molecular organic solar cells as transport layer. Due to its wide band gap, NTCDA does not absorb in the visible range and is furthermore exciton blocking. By doping with AOB (acridine orange base), its conductivity was raised to about $1 \cdot 10^{-4}$S/cm. It can therefore simultaneously be used as electron transport material and optical spacer in p-i-n type solar cells, leading to power conversion efficiencies of up to 2.83%. Additionally, an investigation of the surface morphology using AFM was performed.

Keywords: NTCDA, organic solar cell, electron transport layer, n-type doping

1. INTRODUCTION

Concerning the recent discussions about climate change and the drain on fossile energy resources, the research in the field of renewable energies becomes more and more important. Photovoltaics is one of the most promising environmentally friendly energy sources of the future. Although today the major part of the technology is based on inorganic materials like silicon, the research on organic solar cells (OSCs) has intensified during the last years. Organic devices promise to be comparatively cheap and exhibit some attractive advantages. Due to the high absorbance of organic dyes, thin film thicknesses $\leq$100nm are often sufficient for building efficient photovolatic cells. Therefore, it might be possible to fabricate thin, semitransparent devices onto flexible substrates which could be applied in places inaccessible for the non-flexible inorganic solar cells. Before those visions can be realized, some obstacles concerning long-term stability, power conversion efficiency, encapsulation etc. have to be overcome. At present the benchmark concerning certified efficiencies is set by a polymer solar cell reported by Konarka[1] which yielded η_{PCE} =5.15%.

Our work focusses on organic devices based on small molecules rather than polymers. The cells introduced here are based on the so called p-i-n concept.[2] Here the active intrinsic layers in which the light is absorbed and free charge carriers are generated are embedded between doped organic layers. Such molecular doping results in highly conductive transport regions which guarantee an almost loss-free drain of electrons and holes towards the ITO or metal contacts. In order to increase the efficiency of OSCs not only the properties of the active system have to be optimized but also the properties of the charge transport layers are crucial. While tuning the active heterojunction has important effects on the open circuit voltage V_{oc} and the photocurrent density J_{sc},[3–5] the adjustment of the doped layers mainly influences the fill factor (FF) and again the open circuit voltage of the device.[6] All of the above mentioned features have an impact on the power conversion efficiency η_{PCE} which is given as

$$\eta_{PCE} = \frac{J_{sc} V_{oc} FF}{I_0}. \quad (1)$$

Further author information: (Send correspondence to C.F.)
C.F.: E-mail: Christiane.Falkenberg@iapp.de, Telephone: +49 (0)351 463 35117
K.L.: E-mail: Karl.Leo@iapp.de, Telephone: +49 (0)351 463 37533

Organic Optoelectronics and Photonics III, edited by Paul L. Heremans, Michele Muccini, Eric A. Meulenkamp,
Proc. of SPIE Vol. 6999, 69990S, (2008) · 0277-786X/08/$18 · doi: 10.1117/12.782340

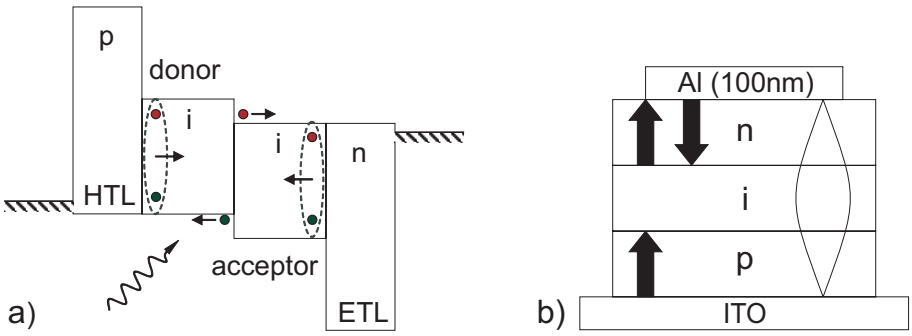

Figure 1. a) P-i-n concept of organic solar cells: excitons are generated within the active donor and acceptor layers by illumination. Due to energy barriers they are unable to pass the interfaces to the neighboring p- or n-layer. At the donor/acceptor heterojunction, the excitons are finally separated into free charge carriers which are then transported towards the electrodes. b) Realization of the p-i-n concept (schematic): Light (outlined by the black arrows) enters the stack through the ITO bottom contact and is reflected at the metal top contact. The maximum of the resulting field distribution can be adjusted to the active layers by thickness variation of the transport layers.

Here I_0 refers to the intensity of the incoupled light which should usually be a standard sun having an AM1.5 (Air Mass) spectrum with 100mW/cm^2 total power density.

While much work is spent on optimizing the active layers, i. e. maximizing the open circuit voltage as well as the photocurrent, this paper will focus on the implementation of proper charge transport layers. They should be composed of materials fulfilling certain criteria like high conductivity, thermal and morphological stability, high charge carrier mobility, transparency, and a good energy level alignment relative to the neighboring active layers. Unfortunately on the side of electron transport (n-side), materials meeting all those requirements are hardly known. Up to now the layer sequence ITO / HTL (hole transport layer) / active system (containing C_{60}) / C_{60} / EBL (electron blocking layer) / Al is used as the standard system here.[7,8] Alternatively OSCs containing an n-C_{60} / Al contact have been fabricated.[9] However, both approaches do not represent the optimum. As will be shown in Sec. 2 choosing the same material – in this case C_{60} – as photoactive material as well as transport material yields certain disadvantages. As a possible substitute for C_{60} as electron transport layer (ETL), this work introduces the transparent electron transporting material 1,4,5,8-naphthalenetetracarboxylic dianhydride (NTCDA). The applicability of undoped NTCDA as thick (600nm...2μm) charge transport and protection layer in organic solar cells has been shown previously by Suemori et al.[10,11] This paper, however, focusses on devices comprising comparatively thin layers of n-doped NTCDA. After discussing some material properties in the first part, we will show the implementation of n-NTCDA as ETL in organic solar cells.

2. PELIMINARY CONSIDERATIONS

Figure 1a) shows the concept of a p-i-n solar cell on which the devices presented in this paper are based on. The active layers in which the absorption of light takes place are positioned in the middle of the stack. Here, excitons are generated, followed by their separation at the active heterojunction between donor and acceptor material. The active area is embedded between the doped charge carrier transport layers which need to be designed as follows: First of all energy level alignment between the transport levels of the adjacent doped and active layers should be obtained in order to avoid energy losses during charge carrier extraction. Secondly, doping ensures that further ohmic losses during the charge transport are minimized. Thirdly, the optical properties of the transport layers represent an important item. The use of so-called widegap materials having a band gap higher than 3eV yields the following advantages: 1.) Since no light is absorbed parasitically in the transport layers, nearly all of the incoupled light intensity reaches the active area. 2.) There is an energy barrier at the interface between active layer and transport layer at which excitons are reflected. Hence the probability of exciton quenching at the dopant molecules or the metal contacs is reduced considerably. 3.) Furthermore, this energy barrier prevents e. g. holes from diffusing into the ETL and therefore works like a selective membrane which ensures a well directed transport. 4.) As Fig. 1b) schematically illustrates, the reflection of the incoupled light (outlined by

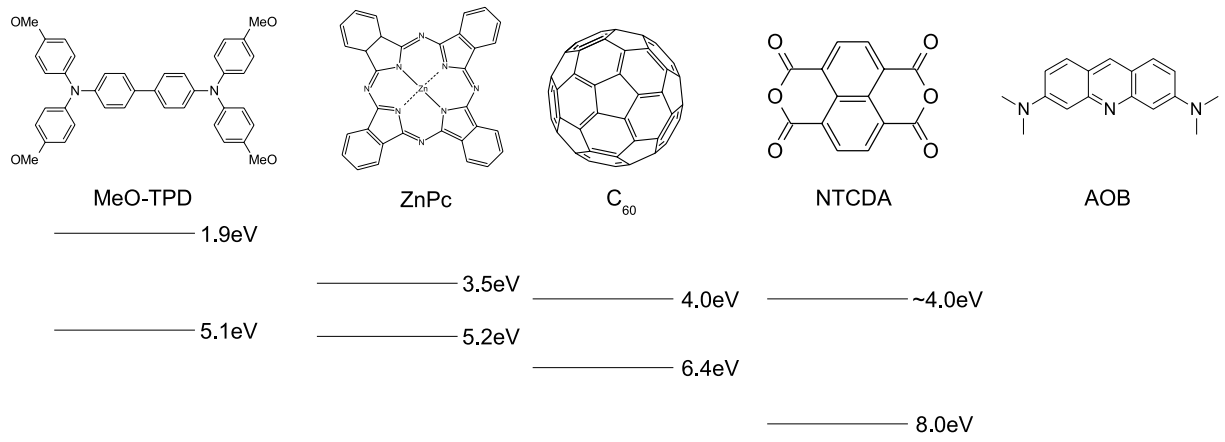

Figure 2. Molecular structure of the materials used: N,N,N',N'-tetrakis(4-methoxyphenyl)-benzidine (MeO-TPD), zinc-phthalocyanine (ZnPc), C_{60}, 1,4,5,8-naphthalenetetracarboxylic dianhydride (NTCDA) and the molecular dopant acridine orange base (AOB) and their HOMO- / LUMO positions.[15–18]

black arrows) at the metal top contact should in the ideal case lead to the formation of a standing wave within the stack. The position of the active layers can now be adjusted to its maximum by means of varying the thickness of the transport layers. Because of the high conductivities, even 100nm thick layers can be used without causing large ohmic losses.[12,13] In addition the insertion of such thick layers prevents the cells from short circuits.

It is obvious that C_{60} fulfills only the first two of the above mentioned criteria for good charge transport layers: energy level alignment relative to the acceptor in the active area (which is not surprising since C_{60} itself usually acts as acceptor) and high conductivity due to doping.[14] Since the LUMO of NTCDA lies with approx. 4.0eV[14,15] close to the LUMO of C_{60}, transport level alignment in the case of NTCDA as ETL is achieved likewise. The deep HOMO of NTCDA (8.0eV[14,15]), however, provides the energy step at the active/ETL interface which is claimed by the p-i-n concept. In the following sections, we discuss whether such a perfect match of energy levels is sufficient for fabricating efficient devices.

3. EXPERIMENTAL SECTION

Materials. The organic semiconductors N,N,N',N'-tetrakis(4-methoxyphenyl)-benzidine (MeO-TPD, Sensient), zinc phthalocyanine (ZnPc, Alpha Aesar), C_{60} (Kurchatov Institute Moscow), 1,4,5,8-naphthalenetetracarboxylic dianhydride (NTCDA, Sigma-Aldrich) and acridine orange base (AOB, Sigma-Aldrich) were purified at least twice by vacuum gradient sublimation before use. The molecular structures are depicted in Fig. 2. At the p-side, the Novaled p-dopant 2 (NDP2) was used instead of 2,3,5,6-tetrafluoro-7,7,8,8-tetracyanoquinodimethan (F_4-TCNQ) due to better thermal stability. At the n-side either the Novaled n-dopant 1 (NDN1) or the conventional n-dopant acridine orange base was chosen. The use of the Novaled dopants does not cause any significant influences on the electronic properties of the devices.

Film Deposition and Characterization. All samples were prepared on precleaned ITO-coated glass substrates (Thin Film Devices Inc., sheet resistance $\leq 30\Omega$/sq) which were treated with organic solvents in an ultrasonic bath. The organic layers were deposited by thermal evaporation at $p < 10^{-6}$mbar and deposition rates of 0.5Å/s in one of two available UHV systems. Either a multi chamber UHV system was used in which the intrinsic layers, all doped layers as well as the metal layers were deposited in separate chambers without breaking the vacuum. Alternatively for OSC fabrication all layers were deposited successively in a single big chamber (K. J. Lesker). Doping was performed by co-evaporation of the dopant and the matrix material from different crucibles whereas the depositon rates were controlled individually by quartz oscillators (Leybold Inficon Inc. Deposition Monitor XTM/2 or Syncon instrument Thickness/Rate Monitor STM-100/MF). The I-V-characteristics of the solar cells were recorded with a Keithley Source Measure Unit (SMU236) in the N_2 athmosphere of a glove box which is directely connected to the vacuum system. The simulated AM1.5 illumination was provided by a

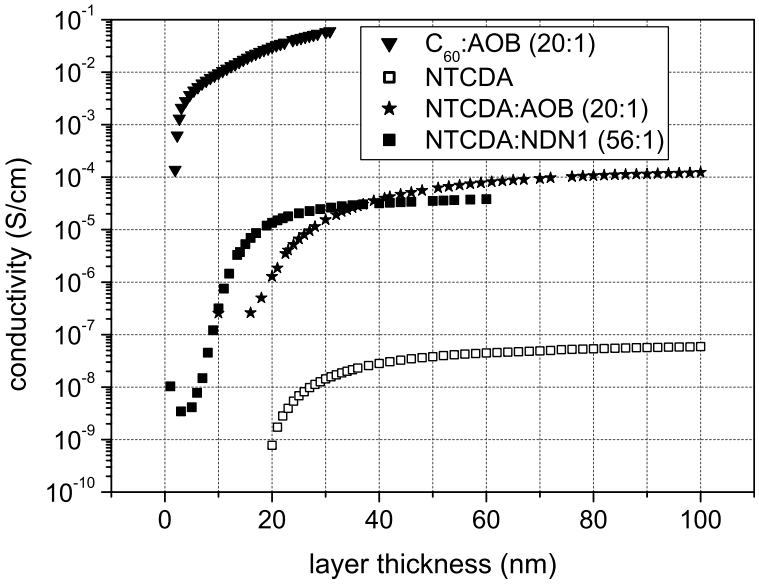

Figure 3. Development of lateral conductivities of doped C_{60} and NTCDA thin-films as a function of the layer thickness. As n-dopants either AOB or NDN1 were used. The doping ratios are given as molar fraction.

sun simulator SOL 1200 (Hoenle AG). An outdoor silicon reference cell from the Fraunhofer Institut für Solare Energiesysteme (Freiburg, Germany) was used to control the intensity at the sample position. A possible spectral mismatch between the simulated and the AM1.5 spectrum or between the spectral responses of reference cell and test cell was not accounted for. The devices have an average active area of 6.6mm^2.

The lateral conductivity was measured by applying a voltage of 10V between two ITO-stripes of the pre-structured solar cell substrates. While depositing an organic layer onto this substrate the current was detected using again a Keithley SMU236.

The morphology of pure NTCDA layers which were deposited on room temperature ITO substrates or thick C_{60} layers was determined with an AFM Nanoscope IIIa (Digital Instruments, Vecco Metrology Group). For comparison such layers were additionally prepared on cooled ITO substrates ($T < -100°$C). All AFM measurements were performed in air shortly after sample preparation.

4. RESULTS

4.1 Characterization of NTCDA

4.1.1 Lateral Conducitvity

The charge carrier density and thus the conductivity can be specifically enhanced by molecular doping.[12,13] For electron transport materials with an electron affinity not higher than 4.0eV (like C_{60} and NTCDA), AOB is an efficient dopant. Alternatively to AOB, the dopant NDN1 was used. As stated above the lateral conductivity of a doped organic layer was detected during the growth of this layer. In the case of isotropic films, this lateral conductivity corresponds to the conductivity perpendicular to the substrate. In Fig. 3 the thickness dependent conductivity of ITO / C_{60}:AOB(19:1, x nm), ITO / NTCDA:AOB(20:1, x nm), ITO / NTCDA:NDN1(56:1, x nm) and ITO / NTCDA(x nm) is displayed on a logarithmic scale. For small layer thicknesses, all curves show a steep slope which corresponds to the growth of the first closed layers. At higher layer thicknesses, the slope decreases significantly and even indicates a saturation in some cases. The conductivity of the C_{60}:AOB film reaches 10^{-2}S/cm at 50nm and militates in favor of superior transport properties of this material. The conductivity of undoped NTCDA approaches 10^{-8}S/cm (at 100nm). By doping with AOB (20:1) or NDN1 (56:1), this value can be increased considerably by 2-3 orders of magnitude and reaches $3.8 \cdot 10^{-5}$S/cm or

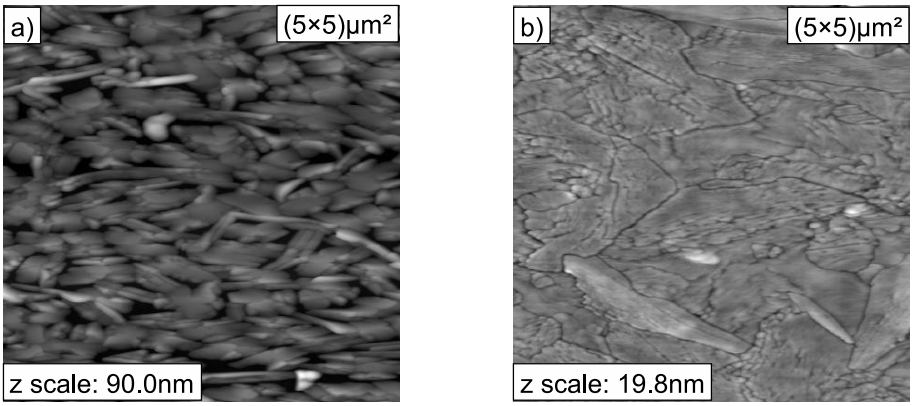

Figure 4. AFM micrographs of a) ITO / NTCDA(22nm) which was prepared on a room temperature substrate and b) ITO / NTCDA(100nm) which was prepared at a substrate temperature of -118°C. At room temperature, NTCDA shows an island growth and forms needle-shaped crystals while it forms smooth layers with a considerably smaller surface roughness upon substrate cooling.

$8.1 \cdot 10^{-5}$S/cm (at 60nm), respectively. Despite the reference value, assigned to doped C_{60}, is still some orders of magnitude higher, those conductivities are sufficient for achieving a good device performance. Furthermore, the shape of the conductivity curves for NTCDA and doped NTCDA is remarkable: the onset of a detectable current through the NTCDA layers starts much later than in the case of n-C_{60} indicating that the formation of a closed layer does not start before a nominal thickness of 5 to 20nm is reached. As will be outlined in Sec. 4.1.2, this hypothesis can be confirmed by atomic force microscopy (AFM) measurements.

4.1.2 Morphological study with AFM

The results obtained for the lateral conductivity of thin films indicate that NTCDA shows an island growth at room temperature. This hypothesis was confirmed by atomic force microscopy (AFM) measurements. As an example, Fig. 4a) shows a $5 \times 5\mu m^2$ AFM micrograph of 22nm NTCDA on ITO. It is clearly visible that the NTCDA layer is not completely closed and the material grows in needle-shaped crystals. The organics covers only about 91% of the substrates surface. Although the nominal layer thickness was only 22nm, an analysis of the AFM picture resulted in an average height of 26.1nm and a root mean square (rms) roughness of 10.9nm. This roughness is comparatively high for an organic layer and leads to considerable problems in device performance when the material is assembled in the middle of the device or at the bottom. Because of the NTCDA morphology such devices tend to have short circuits. Neither the choice of other substrates like metals (Al) or underlying organic layers (C_{60}) nor doping or the coevaporation of NTCDA with C_{60} *and* AOB in order to form an organic alloy[19] led to a reduction of the surface roughness.

Another option for obtaining smoother surfaces is given by substrate cooling during the thin-film preparation. Using nitrogen cooling the substrate temperature was reduced to -118°C during the depositon of a 100nm thick NTCDA film. The resulting surface morphology is depicted in Fig. 4b) and shows smooth domains which are separated by small fosses. Indeed, the average height as well as the rms roughness have dramatically reduced to 9.0nm and 1.5nm, respectively, compared to the films on uncooled substrates. However, for practical implementations this technique might prove to be problematic since the high operation temperatures of solar cells could lead to rapid recrystallisation.

5. SOLAR CELLS COMPRISING NTCDA AS MATRIX MATERIAL FOR ELECTRON TRANSPORT

Several p-i-n OSCs containing different layer thicknesses of NTCDA were prepared in order to prove the applicability of the material as ETL in organic solar cells. The layer structure was chosen as follows: ITO / NDP2(1nm) / p-MeO-TPD(30nm) / ZnPc:C_{60}(37.7nm, 1:1) / C_{60}(26nm) / NTCDA:NDN1(x nm, 20:1) / Al whereas in cell A x=50nm, in cell B x=40nm and in cell C x=30nm. Fig. 5 shows the J-V-curves of all three

Table 1. Light intensity, short circuit current density, open circuit voltage, fill factor, and power conversion efficiency of the reported cell A (comprising 50nm of NTCDA as ETL), cell B (comprising 40nm of NTCDA as ETL) and cell C (comprising 30nm of NTCDA as ETL). The current densities are corrected for 100mW/cm^2 light intensity.

	ETL	I_{sun} (mW/cm^2)	J_{sc} (mA/cm^2)	V_{oc} (V)	FF (%)	η (%)
cell A	50nm n-NTCDA	106.3	10.65	0.52	48.7	2.69
cell B	40nm n-NTCDA	105.8	10.84	0.52	48.7	2.73
cell C	30nm n-NTCDA	106.5	11.41	0.52	47.8	2.83

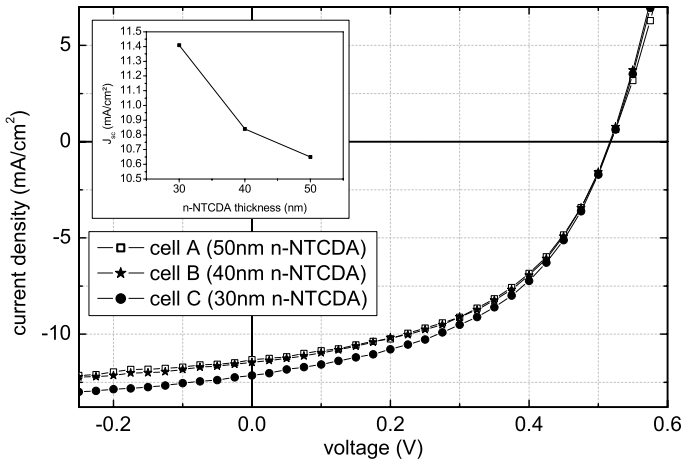

Figure 5. $J-V$-curves of four different solar cells comprising n-NTCDA as electron transport layer: cell A (50nm n-NTCDA), cell B (40nm n-NTCDA) and cell C (30nm n-NTCDA). The inset shows the development of the short circuit current density (corrected for 100mW/cm^2) with increasing ETL thickness.

devices and Table 1 lists the cell parameters. The development of the corrected short circuit current density is depicted in the inset of Fig. 5. With growing ETL-thickness, J_{sc} decreases from $J_{sc,C} = 11.41$mA/cm^2 for cell C to $J_{sc,A} = 10.65$mA/cm^2 for cell A. The open circuit voltage is basically unaffected and the fill factor does not show a clear tendency in favor of any NTCDA film thickness. Consequently, the power conversion efficiency follows the behavior of the current density and increases from $\eta_{PCE,A} = 2.69\%$ for cell A to $\eta_{PCE,C} = 2.83\%$ for cell C. This performance can indeed be explained in terms of the modified p-i-n geometry which changes the distribution of the optical field inside the layer structure. With increasing ETL thickness, the the active area is shifted away from the maximum of the intensity which correlates with a decrease in exciton generation. NTCDA works not only as efficient charge carrier transport layer, but also as optical spacer.

The advantages of transparent transport materials compared to non-transparent materials is shown explicitly in Ref. 14. Upon the exchange of the matrix material of electron transport from n-NTCDA to n-C_{60} in solar cells with identical layer structures an enhancement in power conversion efficiency up to 10% is reached.

Implementing n-NTCDA as ETL in inverted n-i-p structures where it was positioned as bottom layer next to the ITO ground contact failed due to the morphology of the NTCDA films. The growth mode of all organic layers deposited on top of an NTCDA thin-film is influenced considerably leading to short circuits. Hence, it is not possible to use the optical spacer effect of NTCDA in tandem solar cells, unless smoother growth is achieved by suitable techniques.

6. CONCLUSIONS

It was shown that NTCDA meets the requirements for an efficient electron transport material like dopability, high conductivity, thermal stability, and energy level alignment relative to the neighboring layers. However, its morphology represents a drawback: the surface roughness influences the growth of the following layers considerably. Nevertheless, it was possible to build efficient organic solar cells in the p-i-n geometry with an active bulk heterojunction between ZnPc and C_{60}. It was demonstrated that NTCDA works as electron transport layer as well as optical spacer. When comparing identical cell structures which differ only in the choice of the matrix material for the electron transport, an increase in efficiency by 10% is observed upon the exchange of C_{60} by NTCDA. The advantages of widegap materials which were pointed out in Sec. 2 are held responsible for this enhancement.

Though with NTCDA a transparent electron transport material was found which is able to substitue C_{60}, the search for more suitable materials has just started. In order to realize the p-i-n concept properly, having control over the morphology, i. e. the glass transition temperature of organic materials, is important. While NTCDA can only be implemented in the p-i-n geometry, an amorphously growing material could be used just as well in an inverted n-i-p structure or as optical spacer in a tandem solar cell. Since in tandem cells the ETL is embedded in the middle of the stack properties like transparency and smoothness have even larger implications on the efficiency than in single cells. Furthermore, it is of importance to understand how the energy levels can be shifted due to changes in the molecular structure. If in future C_{60} as acceptor material within the active layer might be substitued by another material having different HOMO and LUMO positions. Finding new matrix materials for the ETL which adapt those new conditions will remain a challenge.

ACKNOWLEDGEMENTS

We would like to thank the Bundesministerium für Bildung und Forschung (BMBF) for funding this work within the scope of the Innoprofile project 03IP602.

REFERENCES

1. M. A. Green, K. Emery, Y. Hishikawa, and W. Warta, "Solar cell efficiency tables (version 31)," *Prog. Photovoltaics* **16**, p. 61, 2008.
2. B. Maennig, J. Drechsel, D. Gebeyehu, P. Simon, F. Kozlowski, A. Werner, F. Li, S. Grundmann, S. Sonntag, M. Koch, K. Leo, M. Pfeiffer, H. Hoppe, D. Meissner, N. S. Sariciftci, I. Riedel, V. Dyakonov, and J. Parisi, "Organic p-i-n solar cells," *Appl. Phys. A-Mater.* **79**, p. 1, 2004.
3. M. C. Scharber, D. Wuhlbacher, M. Koppe, P. Denk, C. Waldauf, A. J. Heeger, and C. L. Brabec, "Design rules for donors in bulk-heterojunction solar cells - Towards 10% energy-conversion efficiency," *Adv. Mater.* **18**, p. 789, 2006.
4. S. M. Schultes, P. Sullivan, S. Heutz, B. M. Sanderson, and T. S. Jones, "The role of molecular architecture and layer composition on the properties and performance of CuPc-C-60 photovoltaic devices," *Mat. Sci. Eng. C* **25**, p. 858, 2005.
5. Z. R. Hong, B. Maennig, R. Lessmann, M. Pfeiffer, K. Leo, and P. Simon, "Improved efficiency of zinc phthalocyanine/C-60 based photovoltaic cells via nanoscale interface modification," *Appl. Phys. Lett.* **90**, p. 203505, 2007.
6. C. Uhrich, D. Wynands, M. K. Riede, K. Leo, S. Sonntag, B. Maennig, and M. Pfeiffer, "Origin of open circuit voltage in planar and bulk heterojunction organic thin-film photovoltaics depending on doped transport layers," *J. Appl. Phys.* , submitted.
7. P. Peumans, V. Bulovic, and S. Forrest, "Efficient photon harvesting at high optical intensities in ultrathin organic double-heterostructure photovoltaic diodes," *Appl. Phys. Lett.* **76**, p. 2650, 2000.
8. M. Y. Chan, C. S. Lee, S. L. Lai, M. K. Fung, F. L. Wong, H. Y. Sun, K. M. Lau, and S. T. Lee, "Efficient organic photovoltaic devices using a combination of exciton blocking layer and anodic buffer layer," *J. Appl. Phys.* **100**, p. 094506, 2006.
9. J. Drechsel, B. Maennig, F. Kozlowski, D. Gebeyehu, A. Werner, M. Koch, K. Leo, and M. Pfeiffer, "High efficiency organic solar cells based on single or multiple PIN structures," *Thin Solid Films* **451**, p. 515, 2004.

10. K. Suemori, T. Miyata, M. Yokoyama, and M. Hiramoto, "Three-layered organic solar cells incorporating a nanostructure-optimized phthalocyanine : fullerene codeposited interlayer," *Appl. Phys. Lett.* **86**, p. 063509, 2005.
11. K. Suemori, Y. Matsumura, M. Yokoyama, and M. Hiramoto, "Large area organic solar cells with thick and transparent protection layers," *Jpn. J. Appl. Phys. 2* **45**, p. L472, 2006.
12. M. Pfeiffer, A. Beyer, T. Fritz, and K. Leo, "Controlled doping of phthalocyanine layers by cosublimation with acceptor molecules: A systematic Seebeck and conductivity study," *Appl. Phys. Lett.* **73**, p. 3202, 1998.
13. A. Werner, F. H. Li, K. Harada, M. Pfeiffer, T. Fritz, K. Leo, and S. Machill, "N-type doping of organic thin films using cationic dyes," *Adv. Funct. Mater.* **14**, p. 255, 2004.
14. C. Falkenberg, S. Olthof, M. K. Riede, K. Leo, C. Uhrich, and B. Maennig, "Efficient p-i-n type Organic Solar Cells incorporating 1,4,5,8-Naphthalenetetracarboxylic Dianhydride as Transparent Electron Transport Material," *J. Appl. Phys.* , 2008. (unpublished).
15. C. K. Chan, E. G. Kim, J. L. Bredas, and A. Kahn, "Molecular n-type doping of 1,4,5,8-naphthalene tetracarboxylic dianhydride by pyronin B studied using direct and inverse photoelectron spectroscopies," *Adv. Funct. Mater.* **16**, p. 831, 2006.
16. G. F. He, M. Pfeiffer, K. Leo, M. Hofmann, J. Birnstock, R. Pudzich, and J. Salbeck, "High-efficiency and low-voltage p-i-n electrophosphorescent organic light-emitting diodes with double-emission layers," *Appl. Phys. Lett.* **85**, p. 3911, 2004.
17. W. Y. Gao and A. Kahn, "Effect of electrical doping on molecular level alignment at organic-organic heterojunctions," *Appl. Phys. Lett.* **82**, p. 4815, 2003.
18. O. V. Molodtsova and M. Knupfer, "Electronic properties of the organic semiconductor interfaces CuPc/C-60 and C-60/CuPc," *J. Appl. Phys.* **99**, p. 053704, 2006.
19. T. Mori and Y. Masumoto, "Effect of organic alloy for suppression of polycrystallization in BCP thin film," *J. Photopolym. Sci. Tec.* **19**, p. 209, 2006.